International Journal of Hydrogen Energy xxx (xxxx) xxx

Contents lists available at ScienceDirect

International Journal of Hydrogen Energy

journal homepage: www.elsevier.com/locate/he

The effect of pyrolysis temperature on the optimal conversion of residual biomass to clean syngas through fast-pyrolysis/steam gasification integration

A.A. Papa [a], L. Bartolucci [b], S. Cordiner [b], A. Di Carlo [a], P. Mele [b,*], V. Mulone [b], A. Vitale [a]

[a] Industrial Engineering Department, University of L'Aquila, Piazzale E. Pontieri 1, Monteluco di Roio, 67100, L'Aquila, Italy
[b] Industrial Engineering Department, University of Rome Tor Vergata, Via Del Politecnico 1, Roma, 00133, Roma, Italy

ARTICLE INFO

Handling Editor: Ibrahim Dincer

Keywords:
Biomass
Pyrolysis
Gasification
Tar abatement
Polygeneration energy system
Hydrogen

ABSTRACT

The present work examines the performance of an integrated pyrolysis/gasification energy system, considering biochar as a key element of integration, and assessing the impact of pyrolytic pretreatment on the system behavior. Firstly, softwood pellet (SWP) and spent coffee grounds (SCG) were pyrolyzed using a screw-type reactor in semi-continuous operation (at 400 °C and 500 °C). The steam gasification of biochar at 850 °C was then simulated using a kinetic model based on the results of devolatilization tests performed in a lab-scale fluidized-bed reactor. The results showed that pyrolytic pretreatment significantly reduced tar contamination in the gasification syngas to 0.3g/Nm^3, compared to 24.2 and 18.7g/Nm^3 resulting for raw SCG and SWP, respectively. Furthermore, the comprehensive evaluation of the integrated system confirmed that cold gas efficiency and carbon conversion efficiency of the integrated processes were not affected, despite the different quality of the syngas produced, also highlighting the differences in H_2 production between the two feedstocks.

1. Introduction

As the number of exceptional weather events is increasing due to ongoing climate changes, the importance of limiting the rise in global average temperature to below 1.5 °C is continuously confirmed. In their last energy reports, both IEA and IRENA stressed the importance of achieving net zero CO_2 emissions by 2050 to meet the objectives set by the Paris Agreement in 2015 [1].

In recent years, hydrogen has gained growing interest and is considered a versatile solution for decarbonization across various sectors [2–4]. Despite its promising attributes, hydrogen must address several critical challenges to realize its full potential [5,6]. Currently, 96 % of the hydrogen produced worldwide is from fossil fuels, and the development of sustainable and clean technologies for green hydrogen generation appears crucial [7].

In this context, bioenergy is a key driver to support the energy transition and the development of a hydrogen-based economy [7,8]. Specifically, the bioenergy demand is expected to rise from 55 EJ (in 2019) to more than 150 EJ by 2050 and will represent 25% of the total energy supply. Therefore, research must focus on developing efficient conversion technologies to optimize the effective use of biomass [9,10].

Thermochemical processes allow efficient conversion of the energy potential of residual biomass into valuable bioenergy carriers, which can be used for various purposes, such as combined heat and power generation, industrial heat, hydrogen, and liquid biofuels production [11,12].

Pyrolysis is a thermal depolymerization process for converting feedstock into bio-oil, biochar, and non-condensable gas, carried out in the total absence of oxidizing agents [13]. Operating conditions such as temperature, heat flux, residence time, and inert atmosphere impact process performance and product characteristics [14,15]. In fast pyrolysis, rapid heating of feedstocks with a short residence time of vapors (up to 5 s) at a temperature of 400–500 °C maximizes the bio-oil yield.

Pyrolysis oil is a liquid energy-dense biofuel that can be used for heat and power generation [16]. However, due to its poor physical and chemical properties, water content, and the presence of oxygenated compounds, catalytic upgrading is necessary to use it as a drop-in fuel for transportation applications or as a source of chemicals in a biorefinery [17,18].

Biochar, the solid carbonaceous residue of the pyrolysis process, is a high-quality biomaterial suitable to be used as an enhancer of soil quality [19], as an adsorbent for wastewater treatment, as a precursor of activated carbon [20,21]. Due to its high porosity, electrical

* Corresponding author.
E-mail address: pietro.mele@uniroma2.it (P. Mele).

https://doi.org/10.1016/j.ijhydene.2024.09.100
Received 26 March 2024; Received in revised form 4 September 2024; Accepted 8 September 2024

conductivity, and abundance of functional groups on its surface, biochar can be employed in several electrochemical applications [22,23]. Additionally, its high carbon content (48–89 % by weight) [24] and corresponding high heating value (25–32 MJ/kg) [25] make biochar an energy-dense solid biofuel [26], making its use for energy purposes advantageous in a biomass conversion system.

Gasification is a prominent thermochemical process involving several steps for biomass conversion in high temperatures and oxygen-lacking environments. Thermal decomposition, combined with partial oxidation, facilitates the production of a final gas enriched in H_2 and CO. This gas has a significant potential to generate electricity, to be used for the extraction of biochemicals, produce hydrogen, and synthesize liquid fuels [27,28]. The primary step of gasification is devolatilization. During this phase, the solid material breaks down into many compounds, participating in both homogenous and heterogeneous reactions during gasification [29]. The product distribution is highly influenced by gasification technology and process parameters, i.e. temperature, heating rate, and residence time [28]. Steam gasification process in a fluidized bed reactor is particularly interesting for biomass and waste gasification. Its notable features include high mixing capabilities and superior mass and heat transfer rates, ensuring uniform temperatures throughout the gasifier. However, direct gasification of wet biomass could be inefficient. Furthermore, the tar content significantly affects the usability of syngas in downstream processes [30].

The integration of thermochemical processes has already been identified as an efficient strategy to improve the end-product quality, maximize competitiveness, and increase the economic potential of biomass-derived carriers [31,32].

Several studies have investigated on the benefits of integrating pyrolysis/torrefaction and gasification processes, focusing on improving product quality. Most of these studies were conducted at a laboratory scale, employing fixed-bed reactors to evaluate the hydrogen content in the syngas, the tar reduction, and the conversion efficiency.

In [26], H. Cay et al. studied the two-step steam gasification of spent coffee grounds (SCG) pyrolysis char in a laboratory-scale fixed-bed reactor operated in batch mode at 850 °C [26]. They demonstrated that the pyrolysis pretreatment temperature of 500 °C was optimal for obtaining higher hydrogen yields (up to 2200 mL/g fuel) and a significant reduction in tar contaminants (less than 0.1 % by weight). They attributed the superior performance of biochar gasification to the carbon and ash content of the fuel.

Y. Xin et al. performed the two-step gasification of cattle manure, optimizing the pyrolysis and gasification temperatures to achieve high hydrogen production [33]. They employed a fixed bed reactor operated in batch mode for both processes in the temperature range of 300–600 °C for pyrolysis and 750–850 °C for steam gasification. They found that pyrolytic pretreatment increased hydrogen concentration and yields, respectively up to 57.78% and 0.93 m^3/kg. Furthermore, the gasification temperature of 850 °C produced superior carbon conversion and syngas yield.

J. Huang et al. investigated the effect of torrefaction pretreatment on the gasification performance of starchy food waste [34]. They employed a horizontal fixed-bed reactor for torrefaction and a customized vertical fixed-bed reactor for gasification at 600–1000 °C. The study showed that at lower gasification temperatures (i.e., 700 °C), the raw feedstock showed better carbon conversion and lower tar yields compared to the pre-treated feedstock. Higher temperatures (1000 °C) were required to generate high-quality syngas from torrefied leftover rice and reduced tar yield. Y. Situmorang et al. investigated the steam gasification of pyrolysis char from different feedstocks, highlighting the role of alkali and earth metals for biochar reactivity. They used a fixed bed reactor, operated in semi-batch mode at 500 °C and 750 °C for pyrolysis and steam gasification, respectively. They concluded that biomass selection plays a significant role in achieving efficient two-stage gasification [35].

T. Yu et al. studied the reactivity of residual pruned apple branch biochar in the steam gasification process. They employed a fixed-bed reactor, operated in batch mode, assessing the optimal pretreatment and gasification temperature, the biochar particle size, and the steam flow rate within the process. They found that 550 °C was the optimal pyrolysis temperature for the pretreatment due to the high reactivity of the feedstock with steam. In addition, they showed that at 850 °C, gasification improved syngas and hydrogen yields for all selected steam flow rates and particle sizes [36].

A. Anniwaer et al. investigated the effect of the carbonization pretreatment on the gasification performance of Japonese cedarwood. They obtained that the pretreatment led to higher carbon conversion efficiencies, superior hydrogen yields, and a significant tar reduction. Moreover, they observed a beneficial synergistic effect in the co-gasification of raw feedstock and biochar [37]. In a similar study, A. Anniwaer et al. achieved comparable results for the steam gasification of biochar from Zostera Marina, a marine biomass characterized by significant moisture content and reduced carbon content. Moreover, in this study, the authors also investigated the effect of the calcium oxide physically mixed with the biochar on the gasification performance. They observed that calcium oxide acted as a carbon dioxide absorber, reducing the gasification temperature needed for optimal hydrogen yield [38].

The improvement of torrefaction pretreatment on the gasification performance was also demonstrated at the pilot scale. N. Cerone et al. carried out the air/oxygen/steam gasification of raw and torrefied eucalyptus with a 20 kg/h updraft gasification pilot plant [39]. The results showed that the tar content in the syngas was significantly reduced to 20% of the amount obtained by gasifying the raw feedstock, and the thermal power of the plant was increased by 44%. Furthermore, the cold gas efficiency increased from 75% to 82% in the case of oxygen-steam gasification.

Similarly, a pressurized entrained flow gasification pilot plant, operated at 50 kg/h in the temperature range of 1220–1250 °C, was employed to study the impact of torrefaction on the gasification performance [40]. In this study, both cold gas efficiency and plant efficiency were increased by torrefaction at mild operating conditions.

Considering the aforementioned, torrefaction was already deeply analyzed and demonstrated as an effective pre-treatment to be integrated with gasification at different scales. However, the impact of pyrolysis on gasification performance for lignocellulosic biomass has not been sufficiently investigated, taking into account the actual yield and conversion target of semicontinuous operations.

This study aims, then, at experimentally investigating the interactions between the fast pyrolysis process and steam gasification of residual biomass. Firstly, two lignocellulosic biomass, SWP, and SCG, were pyrolyzed employing a lab-scale screw-type reactor at temperatures of 400 °C and 500 °C. The resulting biochar was then pelletized and devolatilized in a lab-scale fluidized-bed reactor.

The devolatilization tests provide an overview of product distribution, forming the basis for the mathematical modeling of the gasification process [41]. The gasification data obtained from raw and pyrolyzed materials were used to study the integration of the two processes, allowing the analysis of the benefits of pyrolysis pretreatment and the potential use of syngas produced from gasification as an upgrading system for the resulting bio-oil.

This approach, which combines experimental tests of fast pyrolysis in a semi-continuous regime and simulation of steam gasification through kinetic modeling based on devolatilization experimental tests, addresses gaps in the current literature regarding the integration of thermochemical processes. Therefore, this study aims at contributing to the development of energy-driven biorefineries for the valorization of residual biomass through multi-energy carriers.

2. Materials and methods

2.1. Materials

SWP for heating stoves, containing a mixture of softwoods, was used as raw material. SCG (a blend of arabica/robusta 40:60 by weight) were collected from the cafeteria of the Engineering school of Tor Vergata University of Rome. The feedstocks were sieved to obtain a uniform particle size between 500 and 850 μm and dried for 12 h in a conventional oven at 105 ± 1 °C. After drying, both feedstocks were characterized with elemental and proximate analysis. The results of the characterization are reported in Table 1.

2.2. Pyrolysis set-up

Fast pyrolysis of SWP and SCG was carried out employing a 300 g/h screw-type reactor in semi-continuous operation. This reactor configuration was selected to avoid char contamination. The temperature range of 400–500 °C was explored in this study, and the temperature of vapors/gas at the reactor outlet was selected as representative of the process. Nitrogen gas flowed at 0.5 NL/min to ensure an inert atmosphere. A residence time of 15 s for solid particles was measured. Bio-oil was collected using a three-stage condensing system and a solution of water-ethanol (50:50 vol/vol) as a cooler. In the first stage, the condensation takes place in the range of 250-70 °C; in the second stage, the vapors/gas mixture temperature is reduced to 20 °C and in the last stage, to 0 °C. Pyrolysis oil separated spontaneously into organic and aqueous fractions for SCG while it was considered as a single phase for SWP. Biochar and bio-oil yields were measured gravimetrically, while the pyrolysis gas yield was calculated by difference. Further details about the pyrolysis test rig can be found in ref. [43].

2.3. Devolatilization set-up

The devolatilization process was performed using a bubbling fluidized bed reactor, with quartz sand particles having a 2650 kg/m3 density and a Sauter mean diameter of 255 μm. The reactor was externally heated using a 6 kW electric furnace. Fig. 1 reports a full representation of the system used, which is described in detail in a previous work [44].

The experimental tests were carried out according to a pre-defined procedure to determine the gas, char, and tar production for each material. Due to the short residence times of the products in the reactor, homogeneous reactions in the gas phase and the heterogeneous reaction between char and gas can be considered negligible.

In the first step, nitrogen was fed to create an inert environment within the system. The nitrogen flow rate was set to ensure proper fluidization conditions (twice the minimum fluidization velocity) at the fixed operating temperature of 850 °C. Once the target operating conditions were achieved, a batch of the pelletized material was dropped instantaneously in the fluidized bed reactor.

A mass flow meter (MFM) measured the total gas outlet flow rate. The composition of the outlet gases, including carbon dioxide, carbon monoxide, methane, and hydrogen, was detected by ABB analyzers (Caldos and Uras). The heavy hydrocarbon content in the gas phase was also determined by analyzing isopropanol in the impinger bottles downstream of the reactor.

The devolatilization tests were repeated several times for each feedstock. Approximately 10–15 min after the feedstock injection, the next pellet batch was introduced into the fluidized bed. Finally, the combustion step was carried out. During this phase, the air was fed at a fixed flow rate to the reactor, and the flow rate of the gas produced and its composition (in terms of CO and CO_2) were measured. These data were used to determine the amount of char produced during devolatilization and remaining inside the reactor.

Table 1
Feedstock characterization.

	SWP	SCG
Ultimate Analysis (dry basis, in mass percentage (wt. %))		
N	0.03 ± 0.01	1.94 ± 0.25
C	48.5 ± 1.19	51.34 ± 1.13
H	5.2 ± 0.43	6.91 ± 0.65
S	0.06 ± 0.02	0.08 ± 0.02
O[a]	46.04	37.35
Proximate Analysis (dry basis, in mass percentage (wt. %))		
Moisture	5.12 ± 0.08	4.36 ± 0.05
Volatile Matter $_{db.}$	78.88 ± 0.15	76.72 ± 0.07
Fixed Carbon $_{db.}$	20.97 ± 0.11	21.09 ± 0.08
Ash $_{db.}$	0.17 ± 0.01	2.19 ± 0.02
HHV (MJ/kg)[b]	18.91	21.83

[a] Calculated by difference.
[b] Calculated using the following correlation the Dulong expression [42].

2.4. Gasification computational model

The mathematical model used to simulate the gasification phase was previously developed and validated by Di Carlo et al. [45].

Fig. 2 reports a schematic representation of the model, illustrating its rational. The model is based on the Kunnii and Levenspiel approach for describing the behavior of the fluidized bed [46].

The starting point for the simulation is given by the experimental data obtained from the devolatilization tests, which represent the initial phase of the gasification process.

Once the required process conditions were determined, various gasification conditions were analyzed by adjusting the steam-to-carbon ratio for all the feedstocks considered.

2.5. Analytical procedures

The thermogravimetric analysis was carried out according to ASTM E914 using the TGA701 instrument supplied by LECO Corp, and the results were evaluated according to the UNI EN ISO 18122:2016, ISO 18122:2015, and ISO 18123:2015. CHNS(O) analysis was performed with the Elemental Macro's Vario MACRO-cube analyzer. The test and the instrument's calibration with the sulfanilamide standard were carried out according to ISO 16948:2015. Tungsten oxide (WO3) was used as a sorbent to analyze liquid samples. The pyrolysis gas composition was determined with a DANI GC-1000 unit equipped with a ShinCarbon column (ST, 100/120 mesh, 2 m, 1/16in OD, 1.0 mm ID 19808) and a TCD sensor. The HHV of bio-oil and char was calculated based on Dulong expression, knowing the elemental composition [42].

The isopropanol samples collected from the tar sampling unit during the devolatilization tests were analyzed using an Agilent 7890 Gas Chromatograph-Mass Spectrometer (GC-MS) to identify and quantify the content of heavy hydrocarbons in the gas.

2.6. Carbon and energy balance of integrated processes

For the evaluation of the performance of the integrated pyrolysis/gasification energy system, carbon conversion efficiency (CCE) and cold gas efficiency (CGE) were calculated.

CCE was calculated according to Eq. (1).

$$CCE = \frac{c_{CH4} \bullet Y_{CH4} + c_{CO} \bullet Y_{CO} + c_{CO2} \bullet Y_{CO2} + c_{bio-oil} \bullet Y_{bio-oil} + c_{pyr-gas} \bullet Y_{pyr-gas}}{C_{feedstock}} \quad \text{Eq. 1}$$

Where $C_{feedstock}$ is the carbon content of the dried feedstock (SWP or SCG), and c_i and Y_i are the carbon fraction and the yields of the pyrolysis/gasification products.

In detail, the subscripts CH_4, CO, and CO2 refer to the gaseous

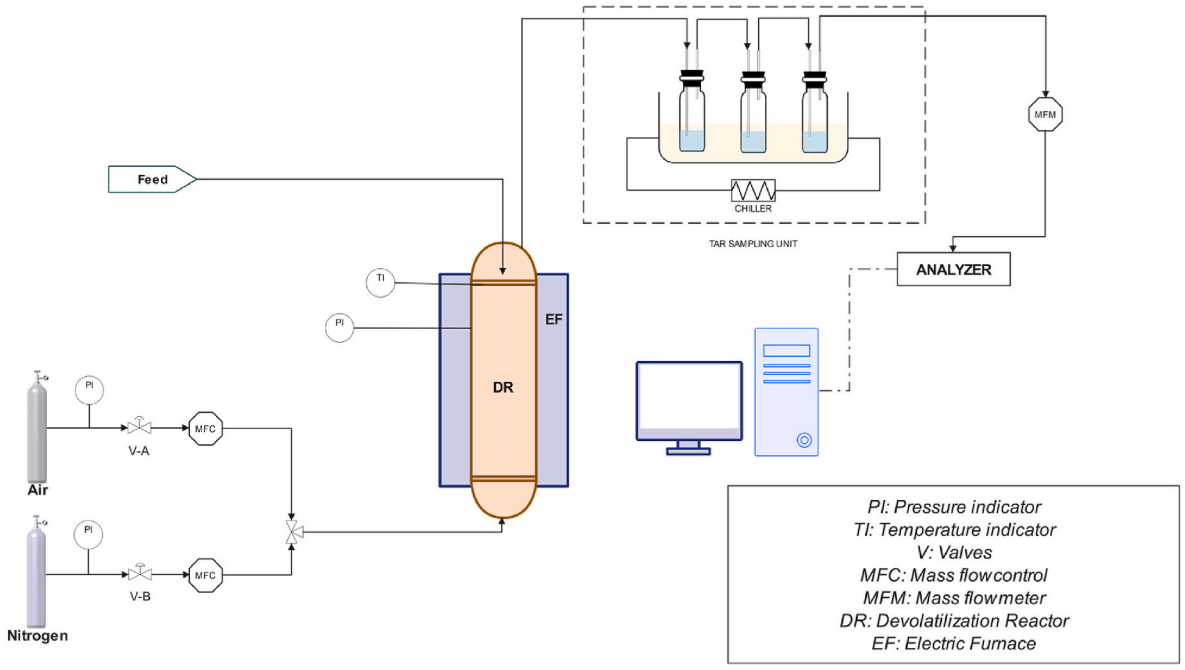

Fig. 1. Schematic representation of the devolatilization test rig.

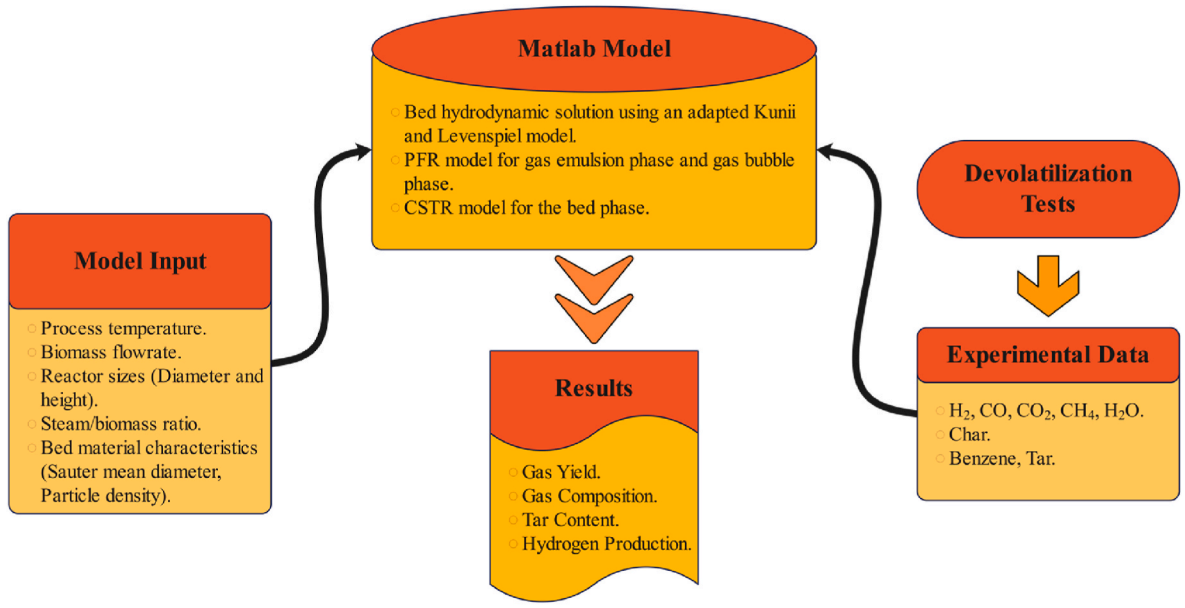

Fig. 2. Schematic representation of the gasification MATLAB model.

species of the gasification process, bio-oil includes both the organic and aqueous fraction of the pyrolysis oil, and pyr-gas refers to the pyrolysis gas.

The CGE was calculated following Eq. (2), according to the definition of CGE reported by Basu [47].

Where HHV_i are the high heating values of the pyrolysis and gasification products. In the expression of CGE, the energy flow of the residual char, after the gasification process does not appear explicitly. However, the energy content of the char is remarkable and was calculated to be sufficient to sustain the energy requirements of the pyrolysis-gasification

$$CGE = \frac{HHV_{H2} \bullet Y_{H2} + HHV_{CH4} \bullet Y_{CH4} + HHV_{CO} \bullet Y_{CO} + HHV_{bio-oil} \bullet Y_{bio-oil} + HHV_{pyr-gas} \bullet Y_{pyr-gas}}{HHV_{feedstock}} \quad \text{Eq. 2}$$

process. Therefore, CGE assumes the meaning of the energy efficiency of the energy system since the processes of gasification and pyrolysis are autothermal.

For the evaluation of the CGE, in the case of SCG, only the organic fraction of the pyrolysis oil was considered since the aqueous fraction is not relevant as an energy carrier. CCE and CGE were calculated for each material, raw and pre-treated at different temperatures, and for different steam-to-carbon ratios (S/C) in the simulations.

3. Results and discussion

3.1. Pyrolysis yields and product characterization

The product yields of SWP and SCG are reported in Fig. 3. The increase of pyrolysis temperature from 400 °C to 500 °C results in a significant decrease in bio-oil yield and an increase in pyrolysis gas production for both feedstocks. This is attributed to the enhanced cracking of volatiles at higherprocess temperatures. Biochar yield undergoes a significant relative reduction with increasing temperature, decreasing from 22.6% to 12.2% for SWP and 27.0% to 18.3% for SCG. The higher values of biochar yield of SCG compared to SWP are related to the higher ash and fixed carbon content, as well as, its greater susceptibility to depolymerization. Several studies have noted that softwood/hardwood feedstocks exhibit faster reaction rates than agricultural residues, mainly due to their less ordered structure and higher oxygen content [48,49].

Similar values of product yields were obtained in previous investigations of fast pyrolysis of SWP and SCG employing auger/screw reactors operating in a semicontinuous regime.

S. Thangalazhy-Gopakumar et al. and S.-S. Liaw et al. observed a significant decrease in biochar yield and an increase in pyrolysis gas production for pine wood/Douglas fir wood in the temperature range 400°C–500 °C [50,51]. Moreover, the yield values of the pyrolysis products in this study are consistent with the previous investigations.

Similarly, Kelkar et al. investigated the effect of temperature and residence time on the product yields SCG pyrolysis employing a screw-type reactor [52]. They obtained similar values for the product yields, whereas the pyrolysis temperature has a lower impact on the yield.

As evident in Fig. 3, pyrolysis oil from SWP appears in a single phase, whereas in the case of SCG, it is fractionated into two distinct phases. The separation of pyrolysis oil into a heavy organic phase and aqueous phases has been widely reported in the literature. Oasmaa et al. examined the multiphase bio-oil behavior from different lignocellulosic biomass. They observed that woody biomass bio-oil generally resulted in a single phase, while for feedstocks with a high ash content and extractives, such as SCG, the pyrolysis oil fractionation occurred [16].

The results of biochar characterization are reported in Fig. 4. Increasing the pyrolysis temperature leads to the progressive thermal degradation of volatiles from biochar and enrichment of fixed carbon and ash for both SWP and SCG. Elemental analysis reveals that the carbon content of SWP and SCG chars increases to 85.7 wt% db. and 78.1 wt % db., respectively. The oxygen content of the biochars is considerably reduced, dropping from 46.0 wt % to 12.49 wt% for SWP and from 37.35 wt% to the 17.21 wt % for SCG. Notably, the oxygen content of SWP biochar is significantly affected by the temperature increase from 400 °C to 500 °C, while for SCG, it keeps stable. Moreover, nitrogen content in SCG chars is relevant, ranging between 2–2.5 wt%, while for SWP, it is negligible.

The pyrolysis oil composition is reported in Table 2. Due to the different structures of the organic and aqueous fractions of the measured SCG pyrolysis oil, the carbon content is very different, i.e., 63.9–67.8 wt % and 10.7–12.4 wt%, respectively. Our previous studies discussed how the bio-oil fractionation is crucial to calculate a reliable value for the carbon and energy balance of the pyrolysis process [53].

For SWP, a single phase of pyrolysis oil is collected, with a carbon content that is in line with the literature [54,55].

The pyrolysis gas composition is shown in Fig. 5. Increasing the pyrolysis temperature leads to an increase in hydrogen concentration and a slight reduction in the carbon dioxide. The enrichment of hydrogen is attributed to enhanced hydrocarbon cracking and the decomposition of lignin at higher temperatures [56]. Thus, the HHV of the pyrolysis gas increases with temperature increase. Similar results on the pyrolysis gas composition were obtained from N. Puy et al. [57] and J.P. Bok et al. [58] for auger/screw pyrolysis of pinewood and SCG, respectively.

3.2. Devolatilization and gasification simulation

As explained above, the raw materials and their corresponding biochars underwent devolatilization tests to analyze the resulting products from the initial phase of the gasification process. Specifically, various pellets of each material were tested to obtain gas and char yields and tar content, as reported in Table 3.

During the pyrolysis process, the fixed carbon content increases, while the volatile content decreases (refer to Fig. 4). The data reported in Table 3 demonstrate that such changes in the characteristics of the substrates are reflected in the behavior observed in devolatilization tests. The gas yield and the tar content decrease by increasing severity of the pyrolysis, while the char yield increases. Furthermore, the gas composition is also affected by the pyrolysis temperature (see Fig. 6); the analysis highlights a reduction in the oxidized compounds, which can be related to the lower O/C ratio of biochar compared to the raw material,

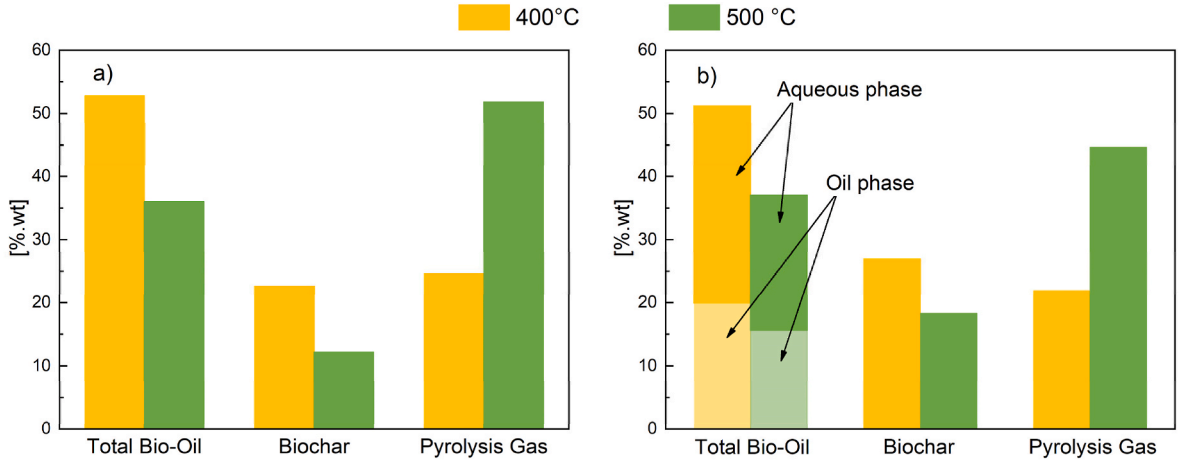

Fig. 3. Pyrolysis product distribution: a) Softwood pellet; b) Spent coffee ground.

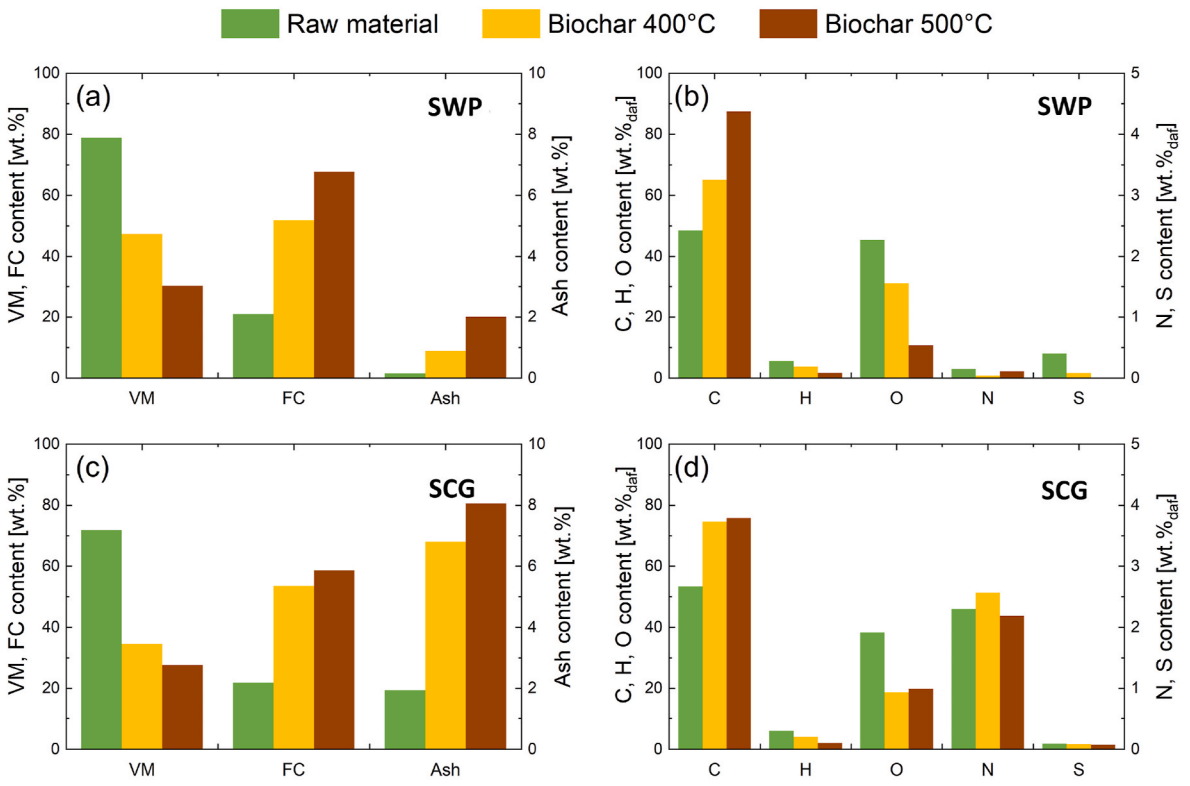

Fig. 4. Comparison of elemental and proximate analysis results of raw and pyrolyzed materials: a) Proximate analysis of softwood pellet; b) Ultimate analysis of softwood pellet; c) Proximate analysis of spent coffee ground, d) Ultimate analysis of spent coffee ground.

Table 2
Pyrolysis oil composition.

Pyrolysis Temperature	400 °C	500 °C
SWP - Bio-oil		
Yield (w/w %)	52.12 ± 2.98	36.01 ± 2.89
C (w/w %)	48.51 ± 3.45	44.22 ± 3.12
H (w/w %)	6.52 ± 1.11	6.15 ± 0.54
N (w/w %)	0.10 ± 0.02	0.20 ± 0.01
S (w/w %)	0.01 ± 0.01	0.02 ± 0.01
O[a] (w/w %)	47.90 ± 4.57	49.54 ± 6.56
HHV[b] (MJ/kg)	18.06 ± 2.16	16.81 ± 2.77
SCG Bio-oil Organic phase		
Yield (w/w %)	19.9 ± 2.13	15.64 ± 1.45
C (w/w %)	63.99 ± 4.98	67.79 ± 3.22
H (w/w %)	11.28 ± 0.45	10.83 ± 0.13
N (w/w %)	1.45 ± 0.12	2.88 ± 0.19
S (w/w %)	0.07 ± 0.01	0.12 ± 0.02
O[a] (w/w %)	23.2 ± 6.73	18.38 ± 5.01
HHV[b] (MJ/kg)	34.75 ± 3.98	36.03 ± 2.76
SCG Bio-oil Aqueous phase		
Yield (w/w %)	31.3 ± 3.41	21.36 ± 2.45
C (w/w %)	12.43 ± 1.02	10.69 ± 1.07
H (w/w %)	10.75 ± 0.63	11.91 ± 0.61
N (w/w %)	1.04 ± 0.10	1.52 ± 0.13
S (w/w %)	0.1 ± 0.01	0.02 ± 0.01
O[a] (w/w %)	75.66 ± 5.14	75.87 ± 4.26
HHV[b] (MJ/kg)	9.81 ± 2.65	10.95 ± 3.12

[a] Calculated by difference.
[b] Calculated using the following correlation the Dulong expression (doi.org/10.1016/S0016-2361(03)00009-7).

along with a decrease in methane content [59].

Significant amounts of methane are released during the pyrolysis process at temperatures higher than 300 °C due to the breakage of alkyl and methoxy group bonds in lignin, leading to a reduction in methane content in devolatilization gas [60,61].

The hydrogen volume fraction in the gas produced by devolatilization of biochar is higher than that obtained from the raw material for both SWP and SCG (see Fig. 6). However, the behavior of the two materials differs when considering hydrogen production per gram of devolatilized material, calculated as the product of gas yield and hydrogen volume fraction. SWP shows a decreasing trend, with hydrogen production reduced by 38% and 60% for Biochar400 and Biochar500, respectively. In contrast, SCG reaches a maximum hydrogen production of 0.212 Nl/g with Biochar400 and shows nearly similar values for both the raw material and Biochar500.

Hiping Yang et al. thoroughly analyzed the effect of pyrolysis on the main biomass constituents (hemicellulose, cellulose, and lignin) using a TGA, providing a comprehensive analysis of their decomposition [56]. The working temperature significantly influences the constituent's decomposition, and, consequently, the distribution of the products. Hemicellulose decomposes at a lower temperature range compared to the other components, while the lignin requires a higher temperature for decomposition.

The release of CO_2 is mainly related to the decomposition of hemicellulose and lignin over a wide range of temperatures, while cellulose contributes only to a small portion; similar behavior is also observable for the CO.

Regarding CH4, the three constituents produce a comparable contribution in its production with a main focus on lower temperatures.

By focusing on the hydrogen production, it increased greatly with temperature increasing and it might be attributed to the higher content of aromatic ring and O–CH_3 functional groups degraded in the lignin as the H_2 from organics pyrolysis mainly came from the cracking and deformation of C═C (ar.) and C–H (ar.) [62].

These considerations can, therefore, justify the results in the figure where treated biomass produces a reduction in the release of CO and CO_2 and an increase of the H_2 term.

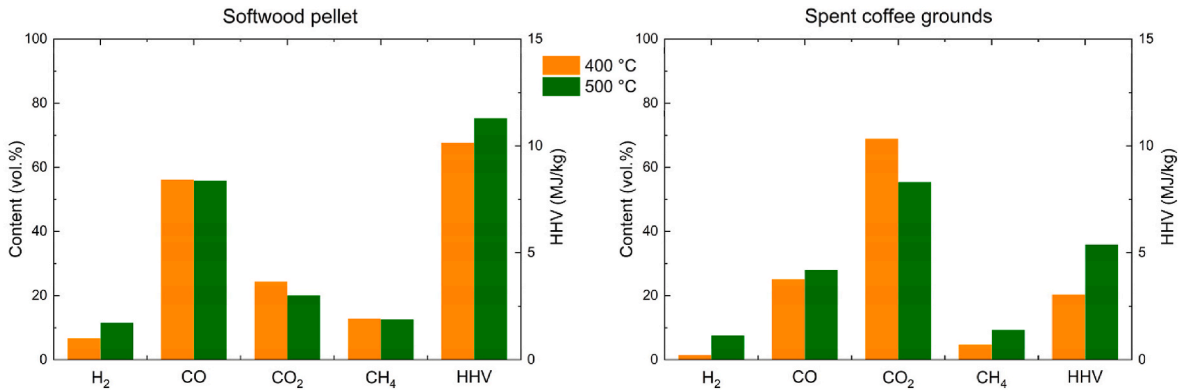

Fig. 5. Pyrolysis gas composition.

Table 3
Summary of the main results of devolatilization tests.

	Gas Yield (Y_G) [Nm^3/kg_{pellet}]	Char Yield (Y_C) [wt. %]	Tar [g/Nm^3]
SWP			
Raw	0.633	10.38	86.9
Biochar400	0.479	32.33	59.9
Biochar500	0.256	60.26	15.5
SCG			
Raw	0.495	11.52	104.3
Biochar400	0.417	38.55	45.4
Biochar500	0.266	54.24	15.5

Furthermore, the difference in the devolatilization gas composition between the biochar obtained from the different feedstocks is directly related to the structure with the highest presence in oxygenated compounds. This is reflected in the higher concentration of CO in SWP devolatilization gas with respect to SGC. Additionally, SCG contains significant amounts of deoxygenated organic compounds (e.g., fatty acids) whose cracking leads to the release of H_2 and CH_4 [63].

As shown in Table 3 and Fig. 7, the tar content decreases by increasing severity of the pyrolysis process. This phenomenon is due to the reduction of volatile substances which, in general, make biomass more susceptible to the formation of tar.

More in detail, tars are the products of cellulose, hemicellulose, and lignin depolymerization, with these reactions starting at temperatures between 250 and 350 °C. Thus, the observed reduction in tar can be attributed to their release during the pyrolysis phase [59].

Table 4 and Fig. 8 present the simulation results obtained using the mathematical model developed in MATLAB, varying the S/C ratio.

These results point out what was observed with the devolatilization tests, showing a substantial reduction in the tar content already for the materials pretreated at 400 °C. A higher S/C ratio would allow for increased utilization of residual char downstream of devolatilization,

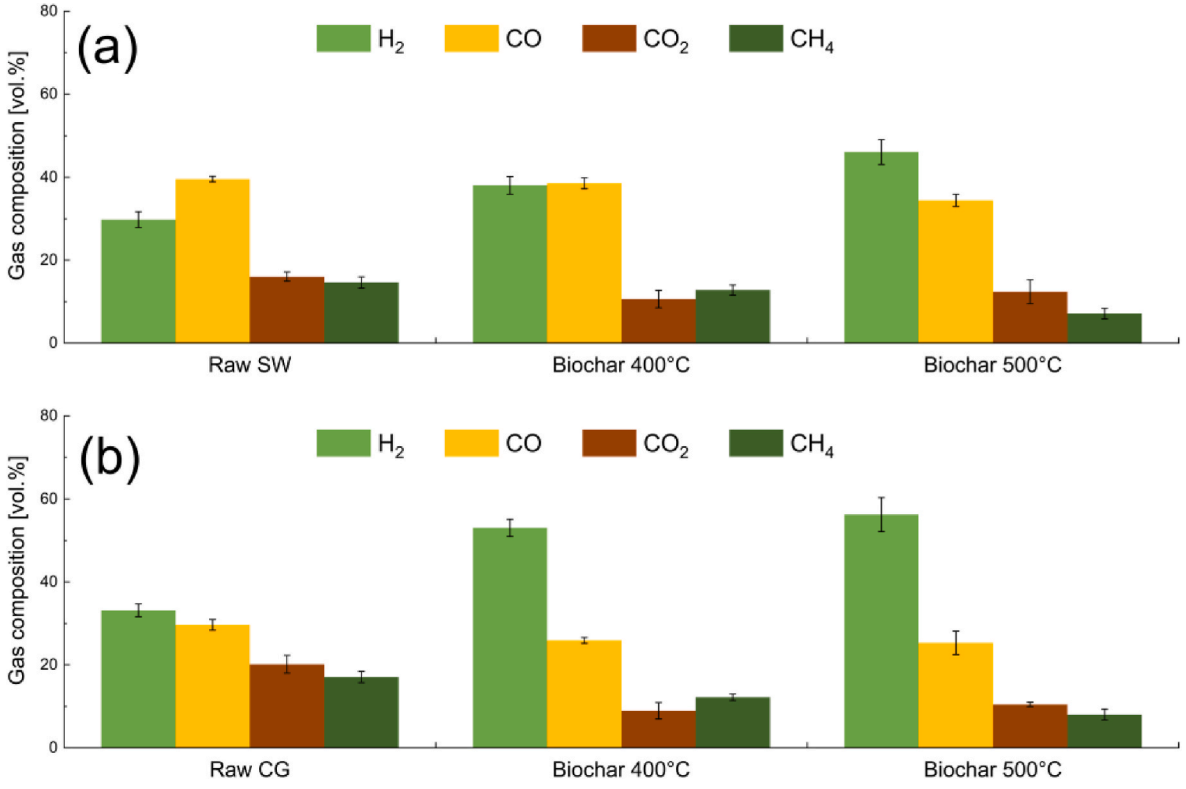

Fig. 6. Devolatilization gas composition with raw material and corresponding biochar: a) Softwood pellet; b) Spent coffee ground.

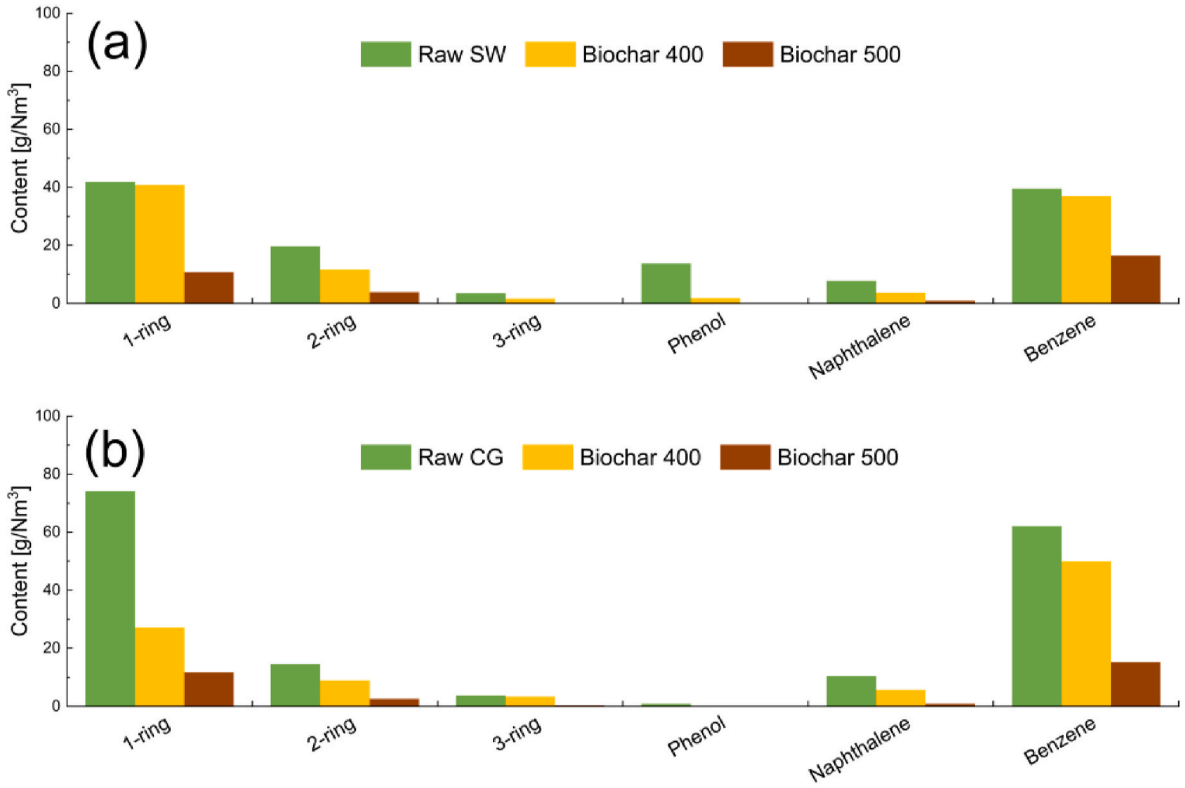

Fig. 7. Devolatilization gas tar and benzene content: a) Softwood pellet; b) Spent coffee ground. Tar compounds still represent the bottleneck of the gasification process. Consequently, reducing their production by pretreatment with pyrolysis can lead to significant outcomes.

Table 4
Summary of the main gasification simulations results related to softwood pellet and spent coffee grounds and their biochar at different S/C.

		Raw			Biochar_400			Biochar_500		
S/C		1	2	3	1	2	3	1	2	3
Softwood pellet										
Y_G	[Nm^3/kg]	1.21	1.43	1.59	1.12	1.52	1.84	1.01	1.63	2.12
Y_C	[g_{Char}/g_{C_IN}]	22.8%	19.0%	15.3%	53.5%	42.5%	33.4%	70.4%	53.9%	41.5%
Tar content	[g/Nm^3]	18.7	10.8	8.0	9.6	4.8	3.7	1.0	0.5	0.3
$Water_{conv}$	[%]	35.9%	30.3%	26.3%	36.8%	34.2%	31.4%	41.4%	40.3%	37.3%
$H_{2,\ Produced}$	[$g_{H2}/kg_{Material}$]	47.8	62.9	73.7	52.8	75.9	94.5	51.5	85.6	112.7
Spent coffee grounds										
Y_G	[Nm^3/kg]	1.16	1.41	1.58	1.04	1.49	1.85	0.94	1.34	1.75
Y_C	[g_{Char}/g_{C_IN}]	26.6%	22.1%	17.9%	63.6%	50.7%	40.1%	72.6%	56.2%	43.7%
Tar content	[g/Nm^3]	24.2	13.5	9.9	6.2	3.1	2.1	1.1	0.5	0.3
$Water_{conv}$	[%]	34.6%	30.1%	26.5%	35.3%	34.5%	32.4%	39.3%	40.3%	37.4%
$H_{2,\ Produced}$	[$g_{H2}/kg_{Material}$]	48.9	64.8	76.2	55.1	80.1	100.7	50.1	72.0	94.8

enhancing hydrogen production through char gasification with steam and WGS reaction. However, the water conversion remains relatively low. Notably, the two materials exhibit different results in hydrogen production, with SCG favored by pyrolysis at 400 °C and SWP at 500 °C.

In any case, the results highlight that coupling pyrolysis and gasification processes improves the syngas quality, potentially reducing reliance on commonly applied catalysts for upgrading. Consequently, industrial gas cleaning units can be downsized [64].

4. Integration

The overall balance of the integrated pyrolysis-gasification process is reported in Tables 5 and 6 for SWP and SCG, respectively. The tables compare the mass flows for the case of the steam gasification of the raw feedstock and with a pyrolysis process pretreatment, at a different S/C ratio. SWP and SCG have similar performance in terms of product yields. As expected, pyrolysis char yield deeply influences the syngas yield, because of the minor amount of material that is fed to the gasification process. Since water conversion slightly decreases with an increase in the S/C ratio within the explored range for both feedstocks, a higher S/C ratio increases syngas yield but has a more pronounced effect on the unreacted water flow. However, the pyrolytic pretreatment leads to better-quality syngas due to the massive reduction of the gasification tar, whose production drops to 0.1 g/kg for both SCG and SWP.

Hydrogen production is in the range of 48–73 g/kg for the raw feedstock, a target in line with what is reported in the literature [39].

Tables 5 and 6 present the CCEs of the proposed integrated pyrolysis-gasification system compared to gasification alone for the two feedstocks. As expected, higher S/C ratios result into higher CCEs for both feedstocks across all cases. The results indicate that integrating

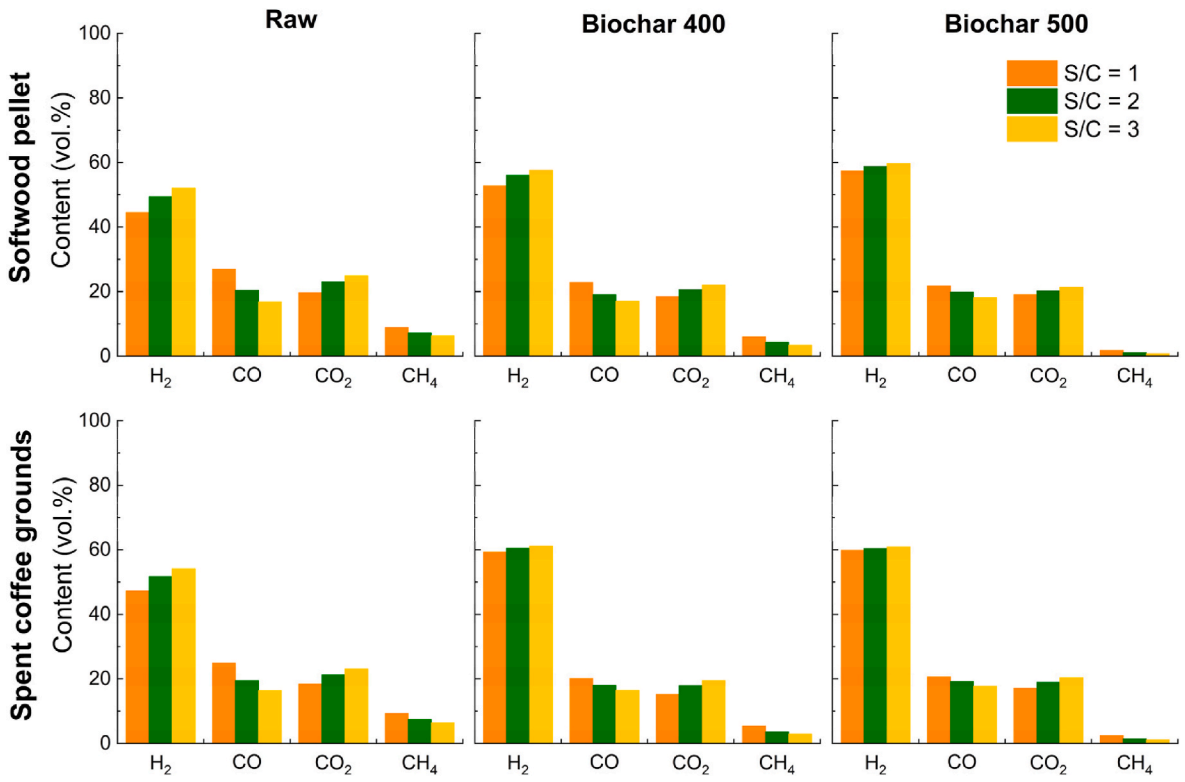

Fig. 8. Syngas composition of gasification simulations related to softwood pellets and spent coffee grounds and their biochar at different temperatures.

Table 5
Overall balance of the integrated processes for softwood wood pellet (SWP).

	Raw			400 °C			500 °C		
Pyrolysis Oil [g/kg]	–	–	–	521	521	521	360	360	360
Pyrolysis Gas [g/kg]				251	251	251	518	518	518
Gasification results									
S/C	1	2	3	1	2	3	1	2	3
$Char_{Residual}$ [g/kg]	113.7	94.7	76.6	77.8	61.8	48.6	66.9	51.2	39.5
Y_G [Nm^3/kg]	1.2	1.4	1.6	0.3	0.3	0.4	0.1	0.2	0.3
Tar [g/kg]	22.6	15.5	12.8	2.5	1.7	1.6	0.1	0.1	0.1
$Water_{Unreacted}$ [g/kg]	353	732	1142	102	201	310	60	120	183
H_2 [g/kg]	48.0	63.0	73.9	12.1	17.4	21.6	6.3	10.4	13.7
CH_4 [g/kg]	76.9	73.5	71.2	11.0	10.6	10.3	1.6	1.5	1.5
CO_2 [g/kg]	466.1	645.8	777.5	92.5	140.5	181.4	45.9	78.8	108.1
CO [g/kg]	405.9	365.2	336.3	73.0	83.1	89.0	33.4	49.4	58.4
CCE	74.0%	80.0%	84.5%	82.5%	86.0%	88.8%	81.1%	84.3%	86.8%
CGE	80%	88%	94%	79%	84%	87%	70%	74%	77%

Table 6
Overall balance of the integrated processes for spent coffee grounds (SCG).

	Raw			400 °C			500 °C		
Pyrolysis Oil (g/kg)	–	–	–	512	512	512	370	370	370
Pyrolysis Gas (g/kg)				219	219	219	447	447	447
Gasification results									
S/C	1	2	3	1	2	3	1	2	3
$Char_{Residual}$ [g/kg]	133.2	110.7	89.6	111.7	89.0	70.4	98.4	76.2	59.3
Y_G [Nm^3/kg]	1.2	1.4	1.6	0.3	0.4	0.5	0.2	0.3	0.4
Tar [g/kg]	28.1	19.0	15.7	1.8	1.3	1.1	0.2	0.1	0.1
$Water_{Unreacted}$ [g/kg]	366	741	1147	120	237	363	86	170	263
H_2 [g/kg]	49.0	65.0	76.4	14.9	21.7	27.3	9.18	15.06	19.81
CH_4 [g/kg]	77.4	74.0	71.8	10.9	10.4	10.2	2.93	2.84	2.8
CO_2 [g/kg]	420.0	588.9	718.3	84.0	140.9	191.5	57.9	104.4	145.9
CO [g/kg]	361.2	342.2	324.0	70.9	90.5	103.0	44.4	67.07	80.50
CCE	63.8%	70.7%	75.7%	57.6%	62.2%	65.9%	60.9%	65.3%	68.6%
CGE	71%	80%	87%	53%	58%	63%	48%	53%	57%

thermochemical processes leads to higher carbon conversion for SWP compared to gasification alone. Notably, for SWP the higher CCEs are obtained in the case of 400 °C of pyrolysis. However, for SWP, both pyrolysis pretreatment temperatures result in better CCEs compared to gasification of the raw material.

In contrast, for SCG, pyrolytic pretreatment leads to lower CCEs. This was attributed to the higher yields of unreacted char in gasification, which are considered as carbon losses in this model, and the lower performance of the SCG pyrolysis.

CGEs are reported in Tables 5 and 6. As evident, process integration results for both feedstocks are less efficient, keeping the same S/C ratios.

As discussed in the previous sections, although the efficiency decreases slightly, the quality of the syngas is significantly improved, in terms of tar concentration and H_2/CO ratio. For both SWP and SCG, a S/C increase leads to a higher CGE, due to an increase in the energy output of the integrated system.

For both feedstocks, a temperature of 400 °C for the pyrolysis process resulted in the most efficient operating conditions in terms of energy conversion.

Previous studies investigated experimentally the impact of the torrefaction pre-treatment on the CGE and CCE of the gasification process. N. Cerone et al. compared the performance of the air/steam and oxygen/steam gasification of raw and torrefied eucalyptus in an updraft gasifier pilot plant [39]. They highlighted how torrefaction pretreatment had a positive effect on the quality of the products with a reduction to about 1/5 of the tar content in the syngas. Moreover, they found that CGE increased in the case of torrefied eucalyptus gasification for raw feedstock.

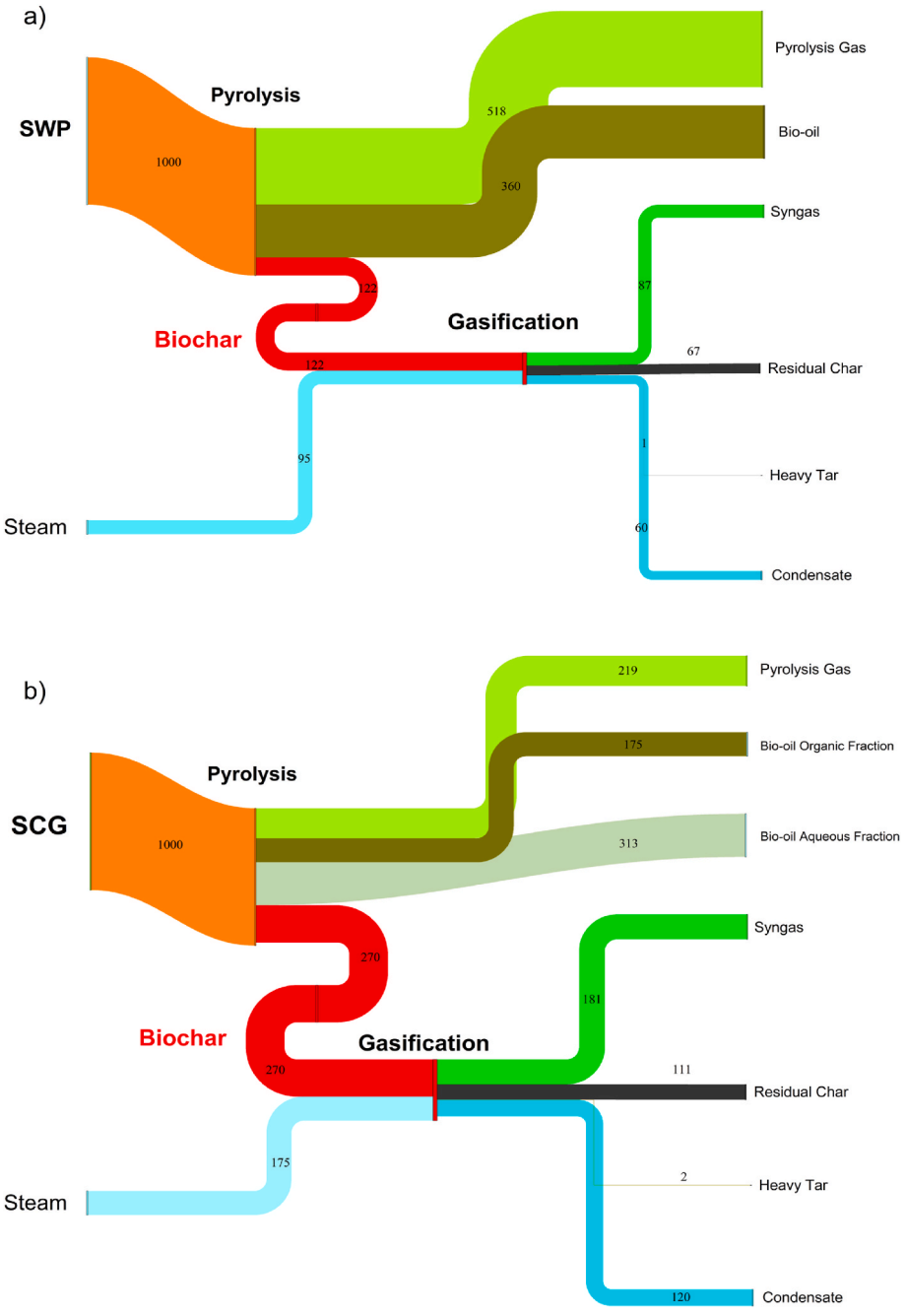

Fig. 9. Sankey diagram of mass flows of integrated pyrolysis/gasification energy system for: a) SWP with pyrolytic pre-treatment at 500 °C, S/C = 1; b) SCG with pyrolytic pre-treatment at 400 °C, S/C = 1. In the figure, each flow is expressed in g/kg of dry feedstock.

M. Di Marcello et al. studied the gasification of torrefied wood employing a pilot-scale steam/oxygen circulating fluidized-bed reactor [65]. They noticed a different behavior of the two woody feedstocks employed: in one case they outlined a reduction of CCE and stable values for CGE in the case of pretreated feedstock, while for the other biomass, the torrefaction led to an increase of both CCE and CGE.

F. Weiland et al. worked on the pressurized entrained-flow gasification of raw/torrefied wood residues in a 270 kW pilot plant [40]. They calculated a higher CGE for all the torrefied feedstock objects of the study, whereas the CCE of the gasification process was affected by the torrefaction operating conditions.

As previously discussed, the CGE assumes the meaning of energy efficiency of the integrated energy system, since the processes of pyrolysis and gasification are considered autothermal. Therefore, this study shows that processes integration leads to lower energy performance of the biomass energy system. It should be noted that the layout of process integration reported in this study was not optimized for energy recovery. Further development of this study will investigate in detail the recovery of waste heat, achieving more accurate results in terms of prediction of energy performance.

Fig. 9 shows a graphical representation of the mass flows of the integrated processes. The Sankey diagrams depict the mass flow rates under optimal operating conditions to produce clean, hydrogen-rich syngas. As discussed in Section 3.2, the biochars from the two feedstocks exhibited different reactivity during devolatilization, leading to varying steam-gasification performance. Specifically, SWP biochar was less reactive than SCG biochar and required a higher pyrolytic pre-treatment temperature to become reactive. Therefore, Fig. 9 (a) reports the mass flows for the integrated pyrolysis-gasification process with pyrolytic pre-treatment at 500 °C for SWP, while Fig. 9 (b) shows the Sankey diagram with pretreatment at 400 °C for SCG. As expected, for SWP, the majority of the system products come from the pyrolytic pre-treatment, with most of the feedstock converted into pyrolysis gas and bio-oil. Overall, the mass flows for steam gasification in SWP are lower, with reduced water consumption and less residual char production. In contrast, the products from steam-gasification of SCG are higher due to the increased feed in the process. As previously mentioned, SCG pyrolysis-gasification system features an additional flow due to the spontaneous fractionation of the pyrolysis oil. Ultimately, the graphical representation of the mass flows reported in Fig. 9 clearly demonstrates that the downstream gasifier should be appropriately sized according to the type of feedstock used in the system.

5. Conclusions

This study aimed at demonstrating the benefits of the integration of pyrolysis and steam gasification for the conversion of residual biomass into valuable syngas and clean hydrogen, providing useful data for the scale-up to an industrial scale. The impact of the pyrolysis temperature and steam/carbon ratio (S/C) for the gasification process on the product yields, the product quality, and the performance of integrated systems (CCE, CGE) was evaluated. The results showed that the proposed concept effectively addresses some of the main challenges of residual biomass gasification, including drastic reductions in the heavy-tar content (down to 0.3 g/Nm^3) and the enrichment of hydrogen content of the syngas (up to 61 % vol/vol). Furthermore, the devolatilization results highlighted different behaviors between the two biochars, indicating that a pyrolytic pre-treatment temperature of 500 °C was necessary for SWP to produce clean syngas, while 400 °C was adequate for SCG. Moreover, the CCE in the case of pyrolytic pre-treatment was higher than for standalone gasification of SWP, reaching up 88.8 % at 400 °C and an S/C of 3. This study reveals the significant influence of feedstock on the selection of optimal operating conditions for the integrated processes, providing valuable insights for the proper sizing of the single process units. Further development of this activity will involve the experimental validation of the concept here proposed, employing a semi-continuous operated fluidized-bed reactor for the steam gasification of pyrolysis char.

CRediT authorship contribution statement

A.A. Papa: Writing – review & editing, Writing – original draft, Visualization, Validation, Software, Methodology, Investigation, Formal analysis, Data curation, Conceptualization. **L. Bartolucci:** Writing – review & editing, Supervision, Resources, Methodology. **S. Cordiner:** Writing – review & editing, Supervision, Resources, Methodology. **A. Di Carlo:** Writing – review & editing, Validation, Supervision, Software, Resources, Methodology. **P. Mele:** Writing – original draft, Methodology, Investigation, Formal analysis, Data curation, Conceptualization. **V. Mulone:** Writing – review & editing, Supervision, Resources, Methodology. **A. Vitale:** Writing – review & editing, Writing – original draft, Visualization, Software, Methodology, Investigation.

Declaration of competing interest

The authors declare the following financial interests/personal relationships which may be considered as potential competing interests:

Armando Vitale reports a relationship with Enereco spa that includes: funding grants. If there are other authors, they declare that they have no known competing financial interests or personal relationships that could have appeared to influence the work reported in this paper.

References

[1] UNFCCC, “Paris Agreement. 21st Conf Parties,” Paris Climate Change Conference - November 2015. Accessed: August. 9, 2021. [Online]. Available: https://unfccc.int/process-and-meetings/the-paris-agreement/the-paris-agreement.

[2] Lee Y, Cho MH, Lee MC, Kim YJ. Policy agenda toward a hydrogen economy: institutional and technological perspectives. Int J Hydrogen Energy Feb. 2024;54:1521–31. https://doi.org/10.1016/J.IJHYDENE.2023.12.129.

[3] Yap J, McLellan B. Exploring transitions to a hydrogen economy: quantitative insights from an expert survey. Int J Hydrogen Energy May 2024;66:371–86. https://doi.org/10.1016/J.IJHYDENE.2024.03.213.

[4] Goren AY, Dincer I, Gogoi SB, Boral P, Patel D. Recent developments on carbon neutrality through carbon dioxide capture and utilization with clean hydrogen for production of alternative fuels for smart cities. Int J Hydrogen Energy Aug. 2024;79:551–78. https://doi.org/10.1016/J.IJHYDENE.2024.06.421.

[5] Koneczna R, Cader J. Towards effective monitoring of hydrogen economy development: a European perspective. Int J Hydrogen Energy Mar. 2024;59:430–46. https://doi.org/10.1016/J.IJHYDENE.2024.02.036.

[6] Palone O, et al. Experimental investigation of thermochemical syngas production in a scrap iron-based oxidizer reactor for industrial decarbonisation. Fuel Sep. 2023;347:128436. https://doi.org/10.1016/J.FUEL.2023.128436.

[7] Khandelwal K, Dalai AK. Integration of hydrothermal gasification with biorefinery processes for efficient production of biofuels and biochemicals. Int J Hydrogen Energy Jan. 2024;49:577–92. https://doi.org/10.1016/J.IJHYDENE.2023.10.337.

[8] Nguyen VG, et al. Recent advances in hydrogen production from biomass waste with a focus on pyrolysis and gasification. Int J Hydrogen Energy Feb. 2024;54:127–60. https://doi.org/10.1016/J.IJHYDENE.2023.05.049.

[9] Lampropoulos A, et al. Techno-economic assessment of an autothermal poly-generation process involving pyrolysis, gasification and SOFC for olive kernel valorization. Int J Hydrogen Energy Dec. 2023;48(99):39463–83. https://doi.org/10.1016/J.IJHYDENE.2023.06.335.

[10] Papa AA, Taglieri L, Gallifuoco A. Hydrothermal carbonization of waste biomass: an experimental comparison between process layouts. Waste Manag 2020;114:72–9. https://doi.org/10.1016/j.wasman.2020.06.031.

[11] Silveira Junior EG, et al. Fast pyrolysis of peanut husk agroindustrial waste: intensification of anhydro sugar (levoglucosan) production. Waste Biomass Valorization Oct. 2021;12(10):5573–85. https://doi.org/10.1007/S12649-021-01403-3/FIGURES/10.

[12] Fytili D, Zabaniotou A. Circular economy synergistic opportunities of decentralized thermochemical systems for bioenergy and biochar production fueled with agro-industrial wastes with environmental sustainability and social acceptance: a review. Current Sustainable/Renewable Energy Reports Jun. 2018;5(2):150–5. https://doi.org/10.1007/S40518-018-0109-5/METRICS.

[13] Volpe M, D'Anna C, Messineo S, Volpe R, Messineo A. Sustainable production of bio-combustibles from pyrolysis of agro-industrial wastes. Sustainability 2014;6:7866–82. https://doi.org/10.3390/SU6117866. vol. 6, no. 11, pp. 7866–7882, Nov. 2014.

[14] Salehi E, Abedi J, Harding T. Bio-oil from sawdust: effect of operating parameters on the yield and quality of pyrolysis products. Energy Fuel Sep. 2011;25(9):4145–54. https://doi.org/10.1021/EF200688Y/ASSET/IMAGES/EF-2011-00688Y_M006.GIF.

[15] Zhang H, et al. Biomass fast pyrolysis in a fluidized bed reactor under N2, CO2, CO, CH4 and H2 atmospheres. Bioresour Technol Mar. 2011;102(5):4258–64. https://doi.org/10.1016/J.BIORTECH.2010.12.075.
[16] Oasmaa A, Fonts I, Pelaez-Samaniego MR, Garcia-Perez MME, Garcia-Perez MME. Pyrolysis oil multiphase behavior and phase stability: a review. Energy Fuel Aug. 2016;30(8):6179–200. https://doi.org/10.1021/ACS.ENERGYFUELS.6B01287/ASSET/IMAGES/LARGE/EF-2016-01287E_0011.JPEG.
[17] Singh PP, Jaswal A, Singh R, Mondal T, Pant KK. Green hydrogen production from biomass – a thermodynamic assessment of the potential of conventional and advanced bio-oil steam reforming processes. Int J Hydrogen Energy Jan. 2024;50:627–39. https://doi.org/10.1016/J.IJHYDENE.2023.10.099.
[18] Koike N, et al. Upgrading of pyrolysis bio-oil using nickel phosphide catalysts. J Catal Jan. 2016;333:115–26. https://doi.org/10.1016/J.JCAT.2015.10.022.
[19] Brassard P, Godbout S, Raghavan V. Soil biochar amendment as a climate change mitigation tool: key parameters and mechanisms involved. J Environ Manag Oct. 2016;181:484–97. https://doi.org/10.1016/J.JENVMAN.2016.06.063.
[20] Chen D, Li Y, Cen K, Luo M, Li H, Lu B. Pyrolysis polygeneration of poplar wood: effect of heating rate and pyrolysis temperature. Bioresour Technol Oct. 2016;218:780–8. https://doi.org/10.1016/J.BIORTECH.2016.07.049.
[21] Weber K, Quicker P. Properties of biochar. Fuel Apr. 2018;217:240–61. https://doi.org/10.1016/J.FUEL.2017.12.054.
[22] Pepè Sciarria T, de Oliveira MAC, Mecheri B, D'Epifanio A, Goldfarb JL, Adani F. Metal-free activated biochar as an oxygen reduction reaction catalyst in single chamber microbial fuel cells. J Power Sources Jun. 2020;462:228183. https://doi.org/10.1016/J.JPOWSOUR.2020.228183.
[23] Monticelli D, et al. Biochar: a sustainable alternative in the development of electrochemical printed platforms. Chemosensors 2022;10. https://doi.org/10.3390/CHEMOSENSORS10080344. 344, vol. 10, no. 8, p. 344, Aug. 2022.
[24] Dhyani V, Bhaskar T. A comprehensive review on the pyrolysis of lignocellulosic biomass. Renew Energy Dec. 2018;129:695–716. https://doi.org/10.1016/J.RENENE.2017.04.035.
[25] Qian C, Li Q, Zhang Z, Wang X, Hu J, Cao W. Prediction of higher heating values of biochar from proximate and ultimate analysis. Fuel Apr. 2020;265:116925. https://doi.org/10.1016/J.FUEL.2019.116925.
[26] Cay H, Duman G, Yanik J. Two-step gasification of biochar for hydrogen-rich gas production: effect of the biochar type and catalyst. Energy Fuel Aug. 2019;33(8):7398–405 [Online]. Available: https://pubs.acs.org/doi/full/10.1021/acs.energyfuels.9b01354. [Accessed 27 June 2023].
[27] Ren J, Liu YL, Zhao XY, Cao JP. Methanation of syngas from biomass gasification: an overview. Int J Hydrogen Energy Feb. 2020;45(7):4223–43. https://doi.org/10.1016/J.IJHYDENE.2019.12.023.
[28] Tezer Ö, Karabağ N, Öngen A, Çolpan CÖ, Ayol A. Biomass gasification for sustainable energy production: a review. Int J Hydrogen Energy Apr. 2022;47(34):15419–33. https://doi.org/10.1016/J.IJHYDENE.2022.02.158.
[29] Kraft S, Kirnbauer F, Hofbauer H. CPFD simulations of an industrial-sized dual fluidized bed steam gasification system of biomass with 8 MW fuel input. Appl Energy Mar. 2017;190:408–20. https://doi.org/10.1016/J.APENERGY.2016.12.113.
[30] Papa AA, Savuto E, Di Carlo A, Tacconi A, Rapagnà S. Synergic effects of bed materials and catalytic filter candle for the conversion of tar during biomass steam gasification. Energies 2023;16:595. https://doi.org/10.3390/EN16020595. vol. 16, no. 2, p. 595, Jan. 2023.
[31] Bartolucci L, et al. Biomass polygeneration system for the thermal conversion of softwood waste into hydrogen and drop-in biofuels. Energies 2023;16:1286. https://doi.org/10.3390/EN16031286. vol. 16, no. 3, p. 1286, Jan. 2023.
[32] Van Nguyen T, Clausen LR. Thermodynamic analysis of polygeneration systems based on catalytic hydropyrolysis for the production of bio-oil and fuels. Energy Convers Manag Sep. 2018;171:1617–38. https://doi.org/10.1016/J.ENCONMAN.2018.06.024.
[33] Xin Y, Cao H, Yuan Q, Wang D. Two-step gasification of cattle manure for hydrogen-rich gas production: effect of biochar preparation temperature and gasification temperature. Waste Manag Oct. 2017;68:618–25. https://doi.org/10.1016/J.WASMAN.2017.06.007.
[34] Huang J, Qiao Y, Wei X, Zhou J, Yu Y, Xu M. Effect of torrefaction on steam gasification of starchy food waste. Fuel Oct. 2019;253:1556–64. https://doi.org/10.1016/J.FUEL.2019.05.142.
[35] Situmorang YA, et al. Steam gasification of co-pyrolysis chars from various types of biomass. Int J Hydrogen Energy Jan. 2021;46(5):3640–50. https://doi.org/10.1016/J.IJHYDENE.2020.10.199.
[36] Yu T, et al. Steam gasification of biochars derived from pruned apple branch with various pyrolysis temperatures. Int J Hydrogen Energy Jul. 2020;45(36):18321–30. https://doi.org/10.1016/J.IJHYDENE.2019.02.226.
[37] Anniwaer A, et al. Steam co-gasification of Japanese cedarwood and its commercial biochar for hydrogen-rich gas production. Int J Hydrogen Energy Oct. 2021;46(70):34587–98. https://doi.org/10.1016/J.IJHYDENE.2021.08.032.
[38] Anniwaer A, et al. Steam gasification of marine biomass and its biochars for hydrogen-rich gas production. Biomass Convers Biorefin Jul. 2023;13(10):8641–50. https://doi.org/10.1007/S13399-020-00868-X/FIGURES/6.
[39] Cerone N, Zimbardi F, Villone A, Strjiugas N, Kiyikci EG. Gasification of wood and torrefied wood with air, oxygen, and steam in a fixed-bed pilot plant. Energy Fuel May 2016;30(5):4034–43. https://doi.org/10.1021/ACS.ENERGYFUELS.6B00126/ASSET/IMAGES/LARGE/EF-2016-00126J_0008.JPEG.
[40] Weiland F, Nordwaeger M, Olofsson I, Wiinikka H, Nordin A. Entrained flow gasification of torrefied wood residues. Fuel Process Technol Sep. 2014;125:51–8. https://doi.org/10.1016/J.FUPROC.2014.03.026.
[41] Vitale A, Di Carlo A, Foscolo PU, Papa AA. Kinetic model implementation of fluidized bed devolatilization. Energies Jun. 2024;17(13):3154. https://doi.org/10.3390/en17133154.
[42] Kathiravale S, Yunus MNM, Sopian K, Samsuddin AH, Rahman RA. Modeling the heating value of municipal solid waste. Fuel Jun. 2003;82(9):1119–25. https://doi.org/10.1016/S0016-2361(03)00009-7.
[43] Bartolucci L, Cordiner S, Mele P, Mulone V. Defatted spent coffee grounds fast pyrolysis polygeneration system: lipid extraction effect on energy yield and products characteristics. Biomass Bioenergy Dec. 2023;179:106974. https://doi.org/10.1016/J.BIOMBIOE.2023.106974.
[44] Vitale A, et al. Devolatilization of polypropylene particles in fluidized bed. Energies 2023;16:6324. https://doi.org/10.3390/EN16176324. vol. 16, no. 17, p. 6324, Aug. 2023.
[45] Di Carlo A, Borello D, Bocci E. Process simulation of a hybrid SOFC/mGT and enriched air/steam fluidized bed gasifier power plant. Int J Hydrogen Energy May 2013;38(14):5857–74. https://doi.org/10.1016/J.IJHYDENE.2013.03.005.
[46] Kunii D, Levenspiel O, Levenspiel O. Fluidized reactor models. 1. For bubbling beds of fine, intermediate, and large particles. 2. For the lean phase: freeboard and fast fluidization. Ind Eng Chem Res Jul. 1990;29(7):1226–34. https://doi.org/10.1021/IE00103A022/ASSET/IE00103A022.FP.PNG_V03.
[47] Basu P. Design of biomass gasifiers. Biomass Gasification Design Handbook Jan. 2010:167–228. https://doi.org/10.1016/B978-0-12-374988-8.00006-4.
[48] Burhenne L, Damiani M, Aicher T. Effect of feedstock water content and pyrolysis temperature on the structure and reactivity of spruce wood char produced in fixed bed pyrolysis. Fuel May 2013;107:836–47. https://doi.org/10.1016/J.FUEL.2013.01.033.
[49] Di Blasi C. Combustion and gasification rates of lignocellulosic chars. Prog Energy Combust Sci Apr. 2009;35(2):121–40. https://doi.org/10.1016/J.PECS.2008.08.001.
[50] Thangalazhy-Gopakumar S, et al. Physiochemical properties of bio-oil produced at various temperatures from pine wood using an auger reactor. Bioresour Technol Nov. 2010;101(21):8389–95. https://doi.org/10.1016/J.BIORTECH.2010.05.040.
[51] Liaw SS, et al. Effect of pyrolysis temperature on the yield and properties of bio-oils obtained from the auger pyrolysis of Douglas Fir wood. J Anal Appl Pyrolysis Jan. 2012;93:52–62. https://doi.org/10.1016/J.JAAP.2011.09.011.
[52] Kelkar S, et al. Pyrolysis of spent coffee grounds using a screw-conveyor reactor. Fuel Process Technol Sep. 2015;137:170–8. https://doi.org/10.1016/J.FUPROC.2015.04.006.
[53] Bartolucci L, Cordiner S, Di Carlo A, Gallifuoco A, Mele P, Mulone V. Platform chemicals recovery from spent coffee grounds aqueous-phase pyrolysis oil. Renew Energy Jan. 2024;220:119630. https://doi.org/10.1016/J.RENENE.2023.119630.
[54] Palacio Lozano DC, et al. Characterization of bio-crude components derived from pyrolysis of soft wood and its esterified product by ultrahigh resolution mass spectrometry and spectroscopic techniques. Fuel Jan. 2020;259:116085. https://doi.org/10.1016/J.FUEL.2019.116085.
[55] Garcìa-Pérez M, Chaala A, Pakdel H, Kretschmer D, Roy C. Vacuum pyrolysis of softwood and hardwood biomass: comparison between product yields and bio-oil properties. J Anal Appl Pyrolysis Jan. 2007;78(1):104–16. https://doi.org/10.1016/J.JAAP.2006.05.003.
[56] Azargohar R, Jacobson KL, Powell EE, Dalai AK. Evaluation of properties of fast pyrolysis products obtained, from Canadian waste biomass. J Anal Appl Pyrolysis Nov. 2013;104:330–40. https://doi.org/10.1016/J.JAAP.2013.06.016.
[57] Puy N, et al. Valorisation of forestry waste by pyrolysis in an auger reactor. Waste Manag Jun. 2011;31(6):1339–49. https://doi.org/10.1016/J.WASMAN.2011.01.020.
[58] Bok JP, Choi HS, Choi YS, Park HC, Kim SJ. Fast pyrolysis of coffee grounds: characteristics of product yields and biocrude oil quality. Energy Nov. 2012;47(1):17–24. https://doi.org/10.1016/J.ENERGY.2012.06.003.
[59] Font Palma C. Modelling of tar formation and evolution for biomass gasification: a review. Appl Energy Nov. 2013;111:129–41. https://doi.org/10.1016/J.APENERGY.2013.04.082.
[60] Umeda K, Nakamura S, Lu D, Yoshikawa K. Biomass gasification employing low-temperature carbonization pretreatment for tar reduction. Biomass Bioenergy Jul. 2019;126:142–9. https://doi.org/10.1016/J.BIOMBIOE.2019.05.002.
[61] Cao J, Xiao G, Xu X, Shen D, Jin B. Study on carbonization of lignin by TG-FTIR and high-temperature carbonization reactor. Fuel Process Technol Feb. 2013;106:41–7. https://doi.org/10.1016/J.FUPROC.2012.06.016.
[62] Quan C, Gao N, Song Q. Pyrolysis of biomass components in a TGA and a fixed-bed reactor: thermochemical behaviors, kinetics, and product characterization. J Anal Appl Pyrolysis Sep. 2016;121:84–92. https://doi.org/10.1016/J.JAAP.2016.07.005.
[63] Bartolucci L, Cordiner S, Mele P, Mulone V. Defatted spent coffee grounds fast pyrolysis polygeneration system: lipid extraction effect on energy yield and products characteristics. Biomass Bioenergy Dec. 2023;179:106974. https://doi.org/10.1016/J.BIOMBIOE.2023.106974.
[64] Di Carlo A, et al. Preliminary results of biomass gasification obtained at pilot scale with an innovative 100 kWth dual bubbling fluidized bed gasifier. Energies 2022;15:4369. https://doi.org/10.3390/EN15124369. vol. 15, no. 12, p. 4369, Jun. 2022.
[65] Di Marcello M, Tsalidis GA, Spinelli G, de Jong W, Kiel JHA. Pilot scale steam-oxygen CFB gasification of commercial torrefied wood pellets. The effect of torrefaction on the gasification performance. Biomass Bioenergy Oct. 2017;105:411–20. https://doi.org/10.1016/J.BIOMBIOE.2017.08.005.